

# The Non-Ergodicity Threshold: Time Scale for Magnetic Reversal

G. L. Celardo,<sup>1</sup> J. Barré,<sup>2</sup> F. Borgonovi,<sup>1,3</sup> and S. Ruffo<sup>4</sup>

<sup>1</sup>*Dipartimento di Matematica e Fisica, Università Cattolica, via Musei 41, 25121 Brescia, Italy*

<sup>2</sup>*Theoretical Division, Los Alamos National Laboratory, USA*

<sup>3</sup>*I.N.F.M., Unità di Brescia and I.N.F.N., Sezione di Pavia, Italy*

<sup>4</sup>*Dipartimento di Energetica “S.Stecch” and CSDC, Università di Firenze, and I.N.F.N., via Santa Marta 3, 50139, Firenze, Italy*

(Dated: January 14, 2019)

We prove the existence of a non-ergodicity threshold for an anisotropic classical Heisenberg model with all-to-all couplings. Below the threshold, the energy surface is disconnected in two components with positive and negative magnetizations respectively. Above, in a fully chaotic regime, magnetization changes sign in a stochastic way and its behavior can be fully characterized by an average magnetization reversal time. We show that statistical mechanics predicts a phase-transition at an energy higher than the non-ergodicity threshold. We assess the dynamical relevance of the latter for finite systems through numerical simulations and analytical calculations. In particular, the time scale for magnetic reversal diverges as a power law at the ergodicity threshold with a size-dependent exponent, which could be a signature of the phenomenon.

PACS numbers: 05.45Pq, 05.45Mt, 03.67,Lx

Statistical mechanics was originally invented to investigate systems with a very large number of weakly interacting particles. Nowadays, as the experimental investigation of few-atoms systems is becoming possible, the analysis of small systems raises fundamental questions [1], and the problem of a statistical description of few-body systems with strongly nonlinear interaction is a subject of current research [2]. Unfortunately we are still far from stating what are the conditions for a few-body system to reach, if any, an equilibrium, and how to describe it, in the same way as statistical mechanics provides a powerful description for  $10^{23}$  particles systems. For instance, even the existence of temperature at the nanoscale has been recently questioned in [3].

Considering that for systems with a few dozens of particles, the range of the interaction is of the same order of magnitude as the whole system [4], we study in this paper finite  $N$  systems with all-to-all coupling. Recently [5], ergodicity breaking has been studied in a finite Heisenberg model with all-to-all spin coupling: below a given specific energy (the non-ergodicity threshold), the magnetization cannot change its sign. On the other hand, above the threshold, as we will show in this Letter, the dynamics can be characterized by a mean reversal time. This type of ergodicity breaking at finite  $N$  is different from the  $N \rightarrow \infty$  ergodicity breaking in a standard Ising model below  $T_c$ , and is expected to be generic in the presence of long range interactions. The main problem is then to provide a theoretical framework to calculate the reversal time [7], a question related to reaction-rate theory (see for instance the Kramer’s model well reviewed in [8]).

Here, we address this issue by investigating the classical dynamics of an anisotropic Heisenberg model, for which a finite number  $N$  of spins interact with all-to-all couplings. As explained above, the all-to-all coupling can be seen as an idealization of a small sample. As an additional motivation, infinite-range interaction terms

have been used in modeling recent experiments on spin chains [9]. The aim is to establish the main physical effects associated with the non-ergodicity threshold with respect to a (statistical) phase-transition appearing at a higher energy. The latter is studied in the microcanonical ensemble, applying a recently developed solution method of mean-field Hamiltonians based on large-deviation theory [10]. These two transitions remain distinct for all  $N$ . A first result presented in this Letter is that the ferromagnetic/paramagnetic transition can be *dynamically driven* below the statistical phase-transition. This happens only in presence of fully chaotic motion. In other words, for all finite  $N$ , an *observation time* exists for which magnetization vanishes in an energy region above the non-ergodicity threshold, and thus below the statistical one. Finally, we give in this Letter an explicit expression for the time scale of *magnetization reversal*. At the ergodicity threshold, this reversal time diverges as a power law, with a characteristic exponent proportional to the number of spins  $N$ , and, based on analytical statistical calculations, we expect this property to be universal close to this type of ergodicity breaking.

The Hamiltonian of the model is

$$H = B \sum_{i=1}^N S_i^z + \frac{J}{2} \sum_{i=1}^N \sum_{j \neq i} (S_i^x S_j^x - S_i^y S_j^y), \quad (1)$$

where  $\vec{S}_i = (S_i^x, S_i^y, S_i^z)$  is the spin vector with continuous components,  $N$  is the number of spins,  $B$  is the rescaled external magnetic field strength and  $J$  the all-to-all coupling strength (the summation is extended over all pairs). Note that the mean field limit of our microscopic spin model, see Eq.(2) below, is formally identical to phenomenological single spin Hamiltonians used to model micromagnetic systems [11]. The equations of motion are derived in a standard way from this Hamiltonian. The total energy  $E = H$  and the spin moduli  $|\vec{S}_i|^2 = 1$

are constants of the motion. Dynamics has been already studied in a similar model [5, 6]. It was found to be characterized by chaotic motion (positive maximal Lyapunov exponent) for not too small energy values and spin coupling constants. For  $J = 0$  the model is exactly integrable, while for generic  $J$  and  $B$  there is a mixed phase space with prevalently chaotic motion for  $|E| \lesssim JN$ .

We will first determine the statistical phase-transition energy of the model in the microcanonical ensemble. The Hamiltonian can be rewritten as

$$H = BNm_z + \frac{J}{2}N^2 (m_x^2 - m_y^2), \quad (2)$$

where  $\vec{m} = (m_x, m_y, m_z) = 1/N \sum_i \vec{S}_i$  and we neglect the term  $J/2 \sum_i (S_i^y)^2 - (S_i^x)^2$ , which is unimportant as far as the statistical properties in the large  $N$  limit, are concerned. The  $N^2$  dependence of the second term is unusual. To deal with it, we introduce a rescaled coupling  $I = JN$ , and we compute the entropy as a function of the order parameter  $\vec{m}$  in the large  $N$  limit (using large deviation techniques [10]). We then extrapolate our results to finite  $N$  as a function of  $J$ . The final results explicitly depend on  $N$ . As illustrated below, this strategy has proved very useful to analyze the system at finite to moderate  $N$  values.

Remarking that in the negative energy range a non-zero value of  $m_x$  is ruled out by entropic considerations, and expressing  $m_z$ , using relation (2), as a function of  $m_y$  and  $\epsilon$ , we obtain the specific entropy as a function of  $m_y$  and  $\epsilon$  only. Then, imposing the vanishing of the second derivative of  $s(m_y, \epsilon)$  at  $m_y = 0$  (a signal of the second order phase-transition) we extract the specific transition energy  $\epsilon_{stat}$ . At the phase-transition the entropy as a function of  $m_y$  changes from a single peaked function to a double-peaked one. For large  $N$  the phase-transition energy density is  $\epsilon_{stat} = -B^2/JN$ . This value is in good agreement with numerical results obtained using (1).

The non-ergodicity energy density  $\epsilon_{ne}$  for the Hamiltonian (1) can be obtained as in Ref. [5]. Even in this case, it is possible to show [12] that the phase space of the system is topologically disconnected below  $\epsilon_{ne}$ . From symmetry considerations both positive and negative regions of  $m_y$  exist on the same energy surface. Switching from a negative  $m_y$  value to a positive one requires, for continuity, to pass through  $m_y = 0$ . Hence, for all energy values above  $\epsilon_{ne} = \text{Min}(\epsilon | m_y = 0)$  magnetization reversal is possible, while below this value magnetization cannot change sign. Computing the minimum, we get [13],

$$\epsilon_{ne} = \begin{cases} -B & \text{for } J \leq B \\ -\left(\frac{B^2}{2J} + \frac{J}{2}\right) & \text{for } J > B. \end{cases} \quad (3)$$

The existence of  $\epsilon_{ne}$  does not represent a sufficient condition in order to demagnetize a sample for  $\epsilon > \epsilon_{ne}$ . Regular structures indeed appear preventing most of trajectories to cross the  $m_y = 0$  plane. The sufficient condition

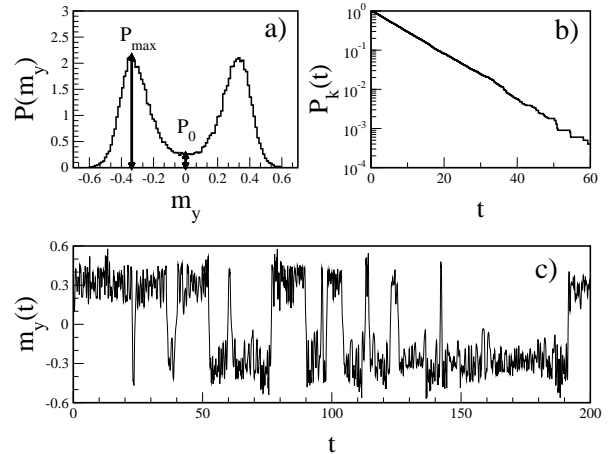


FIG. 1: a) Probability distribution of  $m_y$  for  $\epsilon = -0.9$ . The maximal probability,  $P_{max}$ , and  $P_0 = P(m_y = 0)$  are indicated by vertical arrows. b) Probability of keeping magnetization sign up to time  $t$  vs time. c) Magnetization  $m_y$  vs time. In this figure all data refer to the  $N = 6, B = 1, J = 3$  case.

can only be given by chaos, presumably in the same way as chaos provides the way to break the last golden circle in the standard map, thus allowing transition to global stochasticity [14]. In the following, we will study the dynamics of the full Hamiltonian (1), which, at variance with (2), is non-integrable and displays chaotic motion. Moreover, we will restrict ourselves to the case  $J > B/N$  for which  $\epsilon_{stat} > \epsilon_{ne}$ . The two thresholds  $\epsilon_{ne}$  and  $\epsilon_{stat}$  define three energy regions which show different dynamical and statistical properties.

1) For  $\epsilon < \epsilon_{ne}$ , the probability distribution of  $m_y$ ,  $P(m_y)$ , obtained by a random sampling of constant energy surface [15], shows two separate peaks, with  $P(m_y = 0) = 0$ , so that  $m_y$  cannot change sign in time.

2) For  $\epsilon_{ne} < \epsilon < \epsilon_{stat}$ , the probability distribution is double peaked around the most probable values of the magnetization. These two peaks are not separated and  $P(m_y = 0) \neq 0$ , see Fig. (1a). What actually happens dynamically depends on the relative strength of the coupling  $J$  with respect to  $B$ . For  $J$  large enough the behavior of  $m_y(t)$  resembles a random telegraph noise, (Fig. (1c)): magnetization switches randomly between its two most probable values. The probability distribution of magnetization reversal times follows a Poissonian law,  $P_k(t) \sim e^{-t/\tau}$ , see Fig. (1b), for any initial conditions. Hence, we can characterize the behavior of the system through an average magnetization reversal time  $\tau$ . The Poissonian distribution of the reversal times is a consequence of strong chaos: the system loses its memory due to sensitivity to initial conditions and the reversal probability per unit time becomes time independent. On the contrary, for small  $J$ , we observe a quasi-integrable behavior almost everywhere in the energy range: reversal times strongly depend on initial conditions. Therefore we will limit our considerations to the large  $J$  case.

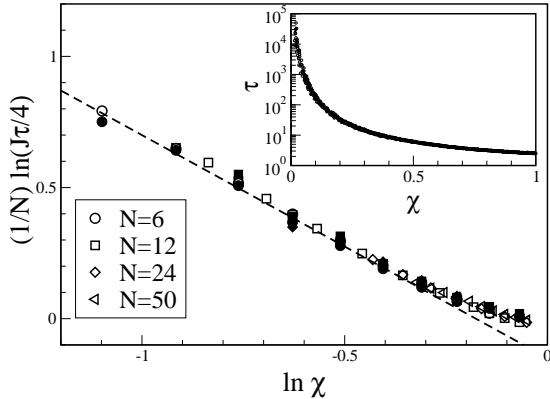


FIG. 2: Average magnetization reversal times  $\tau$  obtained dynamically (open symbols) and statistically (full symbols), *vs* the energy scaling parameter  $\chi = (\epsilon - \epsilon_{ne})/(\epsilon_{stat} - \epsilon_{ne})$  for different  $N$  values and  $B = 0$ . The dynamical determination of  $\tau$  has been obtained by iterating  $10^4$  randomly chosen trajectories for each energy and computing the average reversal time explicitly. The statistical determination of  $\tau$  is obtained from formula (5), where  $P_{max}/P_0$  is numerically determined for each energy density. The dashed line is  $\ln(J\tau/4) = -0.15 - 0.85 \ln \chi$ , where the constants have been obtained through a fitting. Inset : divergence of  $\tau$  at  $\chi = 0$  for  $N = 5$  and  $J = B = 1$ .

3) Finally, for  $\epsilon_{stat} \leq \epsilon \leq 0$ ,  $m_y$  quickly changes sign and  $P(m_y)$  is peaked at  $m_y = 0$ .

For all energies in the range  $(\epsilon_{ne}, \epsilon_{stat})$ , we find that the reversal time  $\tau$  grows exponentially with the number of spins for sufficiently large  $N$ , as expected for mean-field models. More remarkable is the power law divergence of reversal time at the non-ergodicity threshold. Numerical data are consistent with the following scaling law, whose theoretical justification will be given later:

$$\tau \sim \left( \frac{\epsilon - \epsilon_{ne}}{\epsilon_{stat} - \epsilon_{ne}} \right)^{-\alpha N}. \quad (4)$$

Eq. (4) is valid above the non-ergodicity threshold and not too close to the statistical border (observe that  $\chi$  varies in this range between 0 and 1). The comparison of this formula with numerical results is shown in Fig.(2). Let us remark that the reversal time diverges at  $\epsilon_{ne}$ , see the inset of Fig.(2), as a power law, showing that this energy threshold shares many peculiarities with second order phase transitions. In the case  $B = 0$ , we find  $\alpha = 0.85$ , which is at variance with the value  $\alpha = 1$  obtained, for  $N \rightarrow \infty$ , in the mean field approximation (see below). This small discrepancy can be attributed to a finite  $N$  effect. Extensions of these results to the  $B \neq 0$  case show additional dependences of  $\alpha$  on the parameters  $B$  and  $J$  [16]. From Eq. (4) it is also clear that the infinite time average of the magnetization is zero above the non-ergodicity threshold and different from zero below, due to the divergence of the reversal time. Nevertheless, this is not what we obtain during a finite observational time  $\tau_{obs}$ . In Fig.(3) we show the time-averaged magnetization

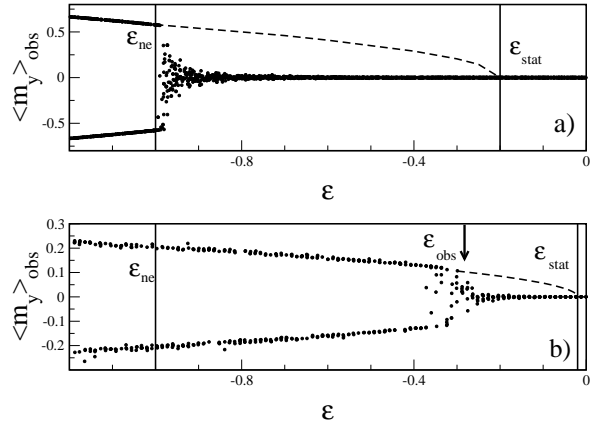


FIG. 3: Time average of  $m_y$  over the observational time  $\tau_{obs}$  *vs*  $\epsilon$  for different number of particles (a)  $N = 5$ , (b)  $N = 50$ , with fixed  $J = B = 1$ . Each single point has been obtained taking the time average over the time intervals  $\tau_{obs} = 10^5$  (a) and  $\tau_{obs} = 10^4$  (b). Dashed curves indicate the equilibrium value of  $m_y$  obtained from statistical mechanics. Vertical lines represent the non-ergodicity and the statistical threshold respectively. The arrow in (b) indicates the energy value  $\epsilon_{obs}$  of the dynamical transition due to the finite observational time.

$\langle m_y \rangle_{obs} = (1/\tau_{obs}) \int_0^{\tau_{obs}} dt m_y(t)$  *vs* the specific energy  $\epsilon$  for  $N = 5$  (Fig.3a) and  $N = 50$  (Fig.3b) spins during a fixed observational time. While in (a)  $\langle m_y \rangle_{obs} \simeq 0$  just above  $\epsilon_{ne}$ , in (b) it vanishes at a value  $\epsilon_{obs}$  located between  $\epsilon_{ne}$  and  $\epsilon_{stat}$ . Indeed, if  $\tau_{obs} \gg \tau$ , the magnetization has time to flip between the two opposite states and, as a consequence,  $\langle m_y \rangle_{obs} \simeq 0$ . On the contrary, if  $\tau_{obs} \ll \tau$  the magnetization keeps its sign and cannot vanish during  $\tau_{obs}$ . Defining an effective transition energy  $\epsilon_{obs}$  from  $\tau_{obs} = \tau(\epsilon_{obs})$ , one gets, inverting Eq. (4), the value indicated by the vertical arrow in Fig. (3b). This is, *a posteriori*, a further demonstration of the validity of Eq. (4) for any  $N$ .

From a theoretical point of view, it is interesting to note that, for any fixed  $N$ , if the fully chaotic regime persists till  $\epsilon_{ne}$ ,  $\epsilon_{obs} \rightarrow \epsilon_{ne}$  when  $\tau_{obs} \rightarrow \infty$ . On the other side, in agreement with statistical mechanics, for any finite  $\tau_{obs}$ ,  $\epsilon_{obs} \rightarrow \epsilon_{stat}$  when  $N \rightarrow \infty$ . This implies that the limits  $\tau_{obs} \rightarrow \infty$  and  $N \rightarrow \infty$  do not commute.

Usually, for long-range interactions, the interaction strength is rescaled in order to keep an extensive energy [17]. In our case this can be done setting  $J = I/N$ . With this choice of  $J$  as  $N \rightarrow \infty$ , at fixed  $I$ ,  $J$  becomes much smaller than  $B$ , then Eq. (4) loses its validity and the quasi-integrable regime sets in. The presence of the non-ergodicity threshold is therefore hidden.

A justification of Eq. (4) can also be given in terms of statistical properties. On the basis of fluctuation theory [18, 19], it has been argued that metastable states relax to the most probable state on times that are proportional to  $\exp(N\Delta s)$  where  $N$  is the number of degrees of freedom and  $\Delta s$  is the specific entropic barrier. In our case  $\exp(N\Delta s)$  is nothing but  $P_{max}/P_0$ , see Fig. (1a). Em-

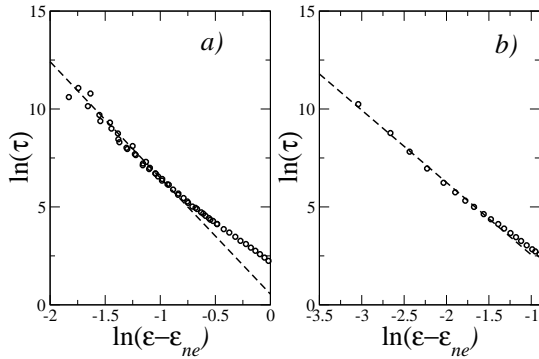


FIG. 4: Reversal time *vs* energy for two different models. a) 3-D cube with an additional spin at the center and nearest neighbor interaction. Best fit gives  $\ln(\tau) \sim -5.9 \ln(\epsilon - \epsilon_{ne})$ , with  $\epsilon_{ne} \simeq -1.33$ , (here  $\epsilon_{min} = -20/9$ ). b) 1-D chain of  $N = 6$  spins with  $r^{-\alpha}$  interaction potential, and  $\alpha = 2$ . Best fit gives  $\ln(\tau) \sim -3.7 \ln(\epsilon - \epsilon_{ne})$ , with  $\epsilon_{ne} \simeq -0.71$ , (here  $\epsilon_{min} = -1.083$ ).

pirically, for  $B = 0$ , we find a very good agreement with the reversal times setting

$$\tau = \text{const.} \times e^{N\Delta s} = \frac{4}{J} \frac{P_{max}}{P_0}. \quad (5)$$

While the  $P_{max}/P_0$  factor in this formula has a theoretical justification, because it represents the probability to cross the entropic barrier, the  $1/J$  factor can be heuristically associated with the typical time scale of the system. A deeper theoretical justification of this formula should be obtained in view of its success in describing the numer-

ical results for different  $N$  values, (Fig.(2)). In the mean field model [12] one has  $P_{max}/P_0 \sim 1/(\epsilon - \epsilon_{ne})^N$ , which reproduces the main feature of Eq. (4) and gives  $\alpha = 1$ . It is also interesting to note the relation with the escape rate from one well for a classical particle moving in a 1-d asymmetric double well potential[8]:  $\lambda \propto \omega_0 \exp(-\beta \Delta E)$  where  $\omega_0$  is the frequency at the bottom of the well,  $\Delta E$  the energy barrier and  $\beta$  the inverse temperature.

Summarizing, the relevance of the ergodicity breaking [5, 7] occurring for any finite  $N$  has been discussed in a long-range spin model. Two distinct energy thresholds are addressed: the non-ergodicity threshold,  $\epsilon_{ne}$ , below which phase space is disconnected and magnetization cannot change sign in time, and the statistical threshold,  $\epsilon_{stat}$ , at which a second order phase-transition occurs in the thermodynamic limit. The non-ergodicity threshold does not disappear in the thermodynamic limit and remains always distinct from the statistical threshold. The results presented in this paper are expected to be valid beyond the toy model studied here. Indeed the existence of the non-ergodicity threshold and the power law divergence of the reversing time have been also found in different small spin systems with a distance-dependent interaction, e.g. 1-D with  $r^{-\alpha}$  interactions potentials and 3-D with nearest neighbor interactions, see Fig.(4).

## I. ACKNOWLEDGMENTS

SR acknowledges financial support under the contract COFIN03 *Order and Chaos in Nonlinear Extended Systems*. Work at Los Alamos National Laboratory is funded by the US Department of Energy. We thank T. Dauxois, E. Locatelli, F. Levyraz, F. M. Izrailev and R. Trasarti-Battistoni for useful discussions.

---

[1] D. H. E. Gross *Microcanonical Thermodynamics: Phase Transitions in Small Systems*, Lecture Notes in Physics **66**, World Scientific, Singapore, 2001.

[2] F. Borgonovi, G. Celardo, F. M. Izrailev, and G. Casati Phys. Rev. Lett., **88**, 054101 (2002); V. V. Flambaum and F. M. Izrailev, Phys. Rev. E, **56**, 5144, (1997); F. Borgonovi and F. M. Izrailev, Phys. Rev. E, **62**, 6475 (2000); F. Borgonovi, I. Guarneri, F.M.Izrailev and G.Casati, Phys. Lett. A, **247**, 140 (1998).

[3] M. Hartmann, G. Mahler and O. Wess. Phys. Rev. Lett. **93**, 80402 (2004).

[4] T. Dauxois, S. Ruffo, E. Arimondo, M. Wilkens Eds., Lect. Notes in Phys., **602**, Springer (2002).

[5] F. Borgonovi, G. L. Celardo, M. Maianti, E. Pedersoli, J. Stat. Phys., **116**, 1435 (2004).

[6] We simulated the dynamic of the system through a Runge Kutta 4-th order integrator.

[7] R. G. Palmer, Adv. in Phys., **31**, 669 (1982).

[8] P. Hanggi, P. Talkner, M. Borkovec, Rev. Mod. Phys. **62**, 2 (1990).

[9] L.Q. English et al., Phys. Rev. B, **67**, 24403 (2003); M. Sato et al., Jour. of Appl. Phys., **91**, 8676 (2002).

[10] R.S. Ellis, Physica D, **133**, 106 (1999); J. Barré, F. Bouchet, T. Dauxois, S. Ruffo, cond-mat/0406358; J. Barré, Phd Thesis, ENS-Lyon, (2003).

[11] E.M.Chudnovsky and J.Tejada, *Macroscopic Quantum Tunneling of the Magnetic Moment*, Cambridge University Press, (1998).

[12] G. L. Celardo, PhD Thesis, Univ. of Milan (2004).

[13] For  $J > B$  the results for odd and even  $N$  coincide up to  $(1/N)$  corrections.

[14] B.V.Chirikov Phys. Rep., **52**, 253 (1979).

[15] Note that the same distribution can be obtained, in a fully chaotic regime, from the time series of  $m_y(t)$ .

[16] When  $J = B$  one has  $\alpha \approx 1/2$ , while for  $J \gg B$ ,  $\alpha$  has the same value as for  $B = 0$ .

[17] M.Kac, G.E.Uhlenbeck and P.C.Hemmer, J. Math. Phys., **4**, 216 (1963).

[18] R. B. Griffiths, C. Y. Weng, and J. S. Langer, Phys. Rev., **149**, 1 (1966); M. Antoni, S. Ruffo and A. Torcini, Europhys. Lett., **66**, 645 (2004); P.H.Chavanis and M.Rieutord Astronomy and Astrophysics, **412**, 1 (2003); P.H.Chavanis, astro-ph/0404251.

[19] L. D. Landau and E. M. Lifshitz, *Statistical Physics* Pergamon Press, Oxford (1985).